Liquid Metal Batteries as a Power Buffer in Aluminium Production Plants

Asbjørn Solheim [1], Karen S. Osen [2], Camilla Sommerseth [2] and Ole E. Kongstein [3]
1. Chief Scientist
2. Research Scientist
3. Senior Research Scientist
SINTEF, Trondheim, Norway
Corresponding author: asbjorn.solheim@sintef.no

Abstract

A new type of liquid metal battery based on sodium and zinc is described. One possible use of such a battery is as a power buffer in an aluminium plant, thus enabling extreme power cycling. By locating the battery in an idled potline, existing infrastructure such as buildings, rectifiers, potshells, and busbars can be utilised. The reversible voltage of the battery is about 1.9 V, and it is suggested to place three battery stacks connected in series to 5.7 V in each potshell of the idle line. By limiting the voltage loss in the electrolyte to 0.15 V per stack at 250 kA, it was estimated that the battery capacity could be about 2.40 MAh, corresponding to 250 kA for 9.6 hours. Provided that the electrolyte height constitutes 50 percent of the total, the stack height will be less than 1.4 m, which can easily be accommodated inside a potshell.

Keywords: Liquid metal battery, aluminium cell, power cycling.

1. Introduction

Rechargeable liquid metal batteries (LMBs) are based on two liquid metals separated by a molten salt [1]. LMBs are attractive due to rapid kinetics, high electrolyte conductivity, only liquid phases (no dendrite formation), and potentially cheap and abundant materials. A new type of membrane free LMB has been suggested [2]. The concept utilises sodium and zinc, while the electrolyte is a ternary mixture of sodium chloride, zinc chloride, and calcium chloride. The battery is intended for use in stationary applications, *e.g.*, for compensation of variable electric power consumption and production in an electric grid based on other energy sources than hydropower, thereby serving to stabilise the grid.

A use case that seems well suited relates to the energy-intensive production of primary aluminium. In many regions, the spot price of electricity varies significantly with time (season, week, day, and hour). Taking Germany as an example; even strongly negative electricity prices have been observed occasionally [3]. Therefore, some aluminium plants are preparing for, experimenting with, and even practising power-cycling (power modulation), *i.e.*, operating the electrolysis cells with reduced power during hours with high energy prices, and increasing the power when the price is low. The energy balance of the electrolysis cells is very delicate however, and the energy window for safe operation is narrow, although variable cooling of the cell sides can be used as a means of increasing the window for power-cycling [4].

The use of an LMB can potentially be an extremely effective strategy for increasing the power-cycling window. The power variation would then be handled by the battery, and not by the electrolysis cells. There are no principal limitations in this type of power-cycling; the only restriction will be the installed battery capacity.

According to data compiled by Pawlek [5], 6.5 Mt/y of the World's total aluminium capacity of 79 Mt/y is idled (2016). Although this includes a number of plants that are entirely closed, it

also means that many plants are operating with one or more shut down potlines. There are a few additional advantages by locating the LMB in a partly closed aluminium plant:

- The building infrastructure is already there.
- The electric bus bars are present.
- The battery can be located in vacant cell positions, perhaps inside electrolysis cell potshells, as was presumed in the present work.
- The rectifier and other electrical infrastructure is in place and may be used as-is or with modifications for charging the battery.
- The personnel in the aluminium plant are aware of and trained for the risks related to handing of liquid metals and molten salts.

3. Principle of the Liquid Metal Battery

A principle sketch of the LMB is shown in Figure 1. The battery contains zinc and sodium, separated by an electrolyte consisting of zinc chloride, sodium chloride, and calcium chloride. The electrolyte is divided in two parts by means of a diaphragm. Detailed descriptions are found below.

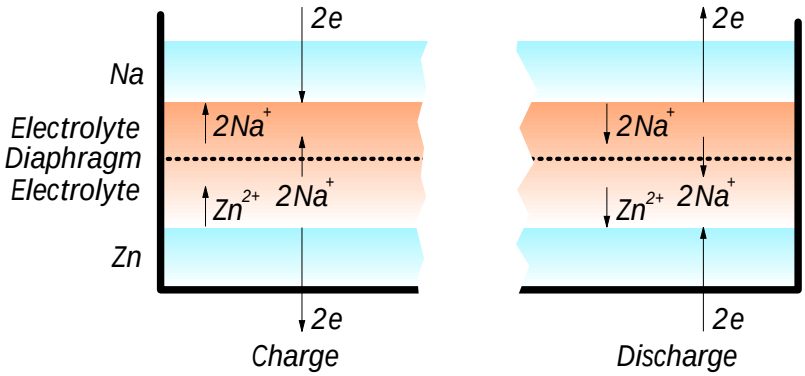

Figure 1. Principle of the liquid metal battery.

3.1. Electrode and Cell Reactions

The electrode reactions (during discharge) are as follows:

$$\text{Sodium electrode}: \quad 2\,\text{Na} + 2\,\text{Cl}^- \rightarrow 2\,\text{NaCl} + 2\,\text{e} \tag{1}$$

$$\text{Zinc electrode}: \quad \text{ZnCl}_2 + 2\,\text{e} \rightarrow \text{Zn} + 2\,\text{Cl}^- \tag{2}$$

The cell reaction is the sum of the two electrode reactions,

$$2\text{Na} + \text{ZnCl}_2 \overset{2\,\text{F}}{=} 2\,\text{NaCl} + \text{Zn} \tag{3}$$

The standard cell voltage for this reaction (E^0, based on Gibbs energy) and the isothermal voltage (E^{iso}, based on the enthalpy change) are +1.914 V and +2.170 V at 600 °C, respectively [6]. The reversible voltage (E^{rev}) is related to the activities of the substances in Equation 3:

$$E^{rev} = E^0 - \frac{RT}{2\,F} \ln\left(\frac{a_{NaCl}^2 \cdot a_{Zn}}{a_{ZnCl_2} \cdot a_{Na}^2}\right) \tag{4}$$

where: *R* Universal gas constant (8.3143 J/mol),
T Temperature (K) and
F Faraday's constant (96485 As/mol).

The activities of the metals can be assumed to be one. During charging the activity of $ZnCl_2$ increases, which causes the (absolute value of) the reversible voltage to increase. The activity of NaCl in the sodium chamber does probably not vary much; see the discussion in Section 3.2 below. It will be possible to keep the reversible voltage within relatively narrow limits, *e.g.*, 1.9 ± 0.05 V, by avoiding full depletion of $ZnCl_2$ during discharge.

3.2. Diaphragm

Any zinc ions present in the electrolyte at the sodium electrode during charging will immediately be reduced, forming a Na-Zn alloy. Without using a membrane or diaphragm, the $ZnCl_2$ formed at the zinc electrode would easily be transported to the sodium electrode by convection. Ideally, a sodium-conducting membrane should be used, such as β-alumina, which is used in NaS and ZEBRA batteries today. However, there are serious challenges related to β-alumina, such as brittleness, high cost, and low conductivity in the presence of zinc [7]. For these reasons, β-alumina was replaced by a diaphragm. A passive diaphragm eliminates convection, but transport between the two electrolyte chambers can still take place by diffusion and migration. Calcium chloride as well as zinc chloride will probably mainly be present in the form of anion complexes with low mobility, so most of the current will be transported by the sodium ion as indicated in Figure 1. This also entails that both the composition and the amounts of electrolyte in the sodium chamber stay almost constant. Nevertheless, some zinc will be reduced into the sodium electrode, which represents a loss in current efficiency.

Zinc and sodium form two immiscible liquid phases. According to the Na-Zn phase diagram by Cetin and Ross [8], the composition of the two phases at 900 K (627 °C) are approximately 19Zn-81Na and 89Zn-11Na on a molar basis. After saturation of the low-Zn alloy due to reduction of Zn^{2+}, the Zn-rich alloy will precipitate and form droplets (possibly during discharge, when Na is oxidised and disappears). Therefore, the diaphragm must be supplied with openings, or made of a coarse material that wets the droplets. The sodium that finds its way to the zinc chamber oxidizes in the zinc chamber, forming NaCl and Zn.

3.3. Electrolyte

As mentioned, the electrolyte contains NaCl, $ZnCl_2$, and $CaCl_2$. The reason for using $CaCl_2$ is to keep the liquidus temperature below 900 K. It may be possible to add LiCl to increase the electrical conductivity of the solution.

The electrolyte in the sodium chamber consists of NaCl and $CaCl_2$, and its composition stays more or less constant during a battery cycle. According to the phase diagram by Robelin and Chartrand [9], the mixture will have liquidus temperatures below 900 K when the concentration of NaCl is between 32 and 63 mol%, as shown in Figure 2. The latter concentration is chosen because of the higher conductivity. The lower electrolyte (zinc chamber) will then contain only 63NaCl-37$CaCl_2$ when the battery is completely discharged. Upon charging to maximum capacity, the composition will change to 46$ZnCl_2$-54$CaCl_2$ (see Figure 2), and the NaCl-$ZnCl_2$-$CaCl_2$ mixture will be liquid during the entire charging process.

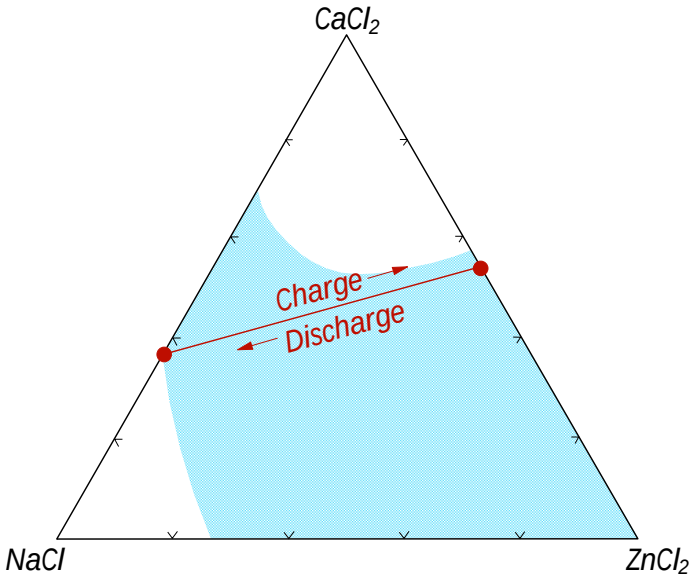

Figure 2. Schematic phase diagram based on Robelin and Chartrand [9]. The shaded area represents the region where the liquidus temperature is below 900 K.

4. Integration in an Aluminium Plant

We assume that the aluminium plant has at least two potlines, of which one has been idled. The batteries are placed in the vacant electrolysis cell positions, utilizing the potshells, bus bars, and the rectifier. As an example, we assume that the two potlines originally had 250 cells each, running at 250 kA and 4.4 V. LMB batteries replace the electrolysis cells in most of the vacant positions in the idled line.

A possible way of connecting the batteries and the neighbouring potline is shown in Figure 3. By using the DC current from the battery directly for the aluminium electrolysis, it is not necessary to acquire an expensive DC-DC converter. In the figure, the battery line is represented by the DC voltage source E_b in series with the resistance R_b, while the electrolysis line is represented by E_p and R_p. The voltage sources comprise reversible voltages and activation overvoltages (the latter are approximately constant). During discharge, the current from the battery (I_b) is combined with the current from the rectifier (I_{pr}) at point *a'* as shown in the figure. Changing from discharge to charge is represented by activating the switch at point *a* (it is not trivial to make and break contact with large currents, so the switching may represent a major challenge).

Since the voltage drop between the points *a* and *b* is the same as between *a*' and *b*', the following applies:

$$E_p + (I_{pr} + I_b)R_p = E_b - I_b R_b \quad (5)$$

Provided that the potline current $I_p = I_{pr} + I_b$ is constant, Equation 5 can be rearranged to express the battery current:

$$I_b = \frac{E_b - E_p - I_p R_p}{R_b} \quad (6)$$

The reversible voltage of the battery is typically 1.9 V. It will, therefore, be beneficial to locate three battery stacks in series in each former electrolysis cell position to obtain a total of 5.7 V, as illustrated in Figure 4.

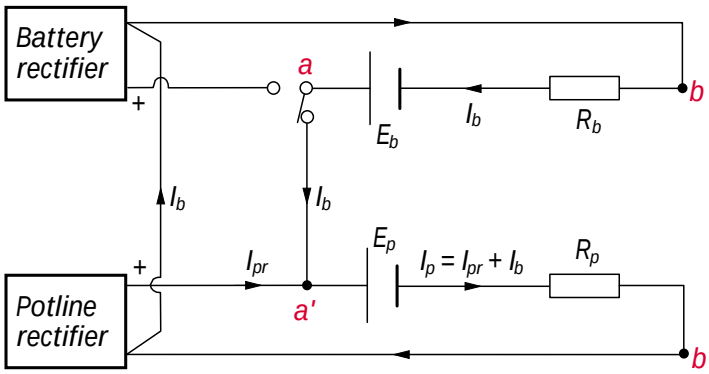

Figure 3. Electrical connections between a potline and a battery during discharge.

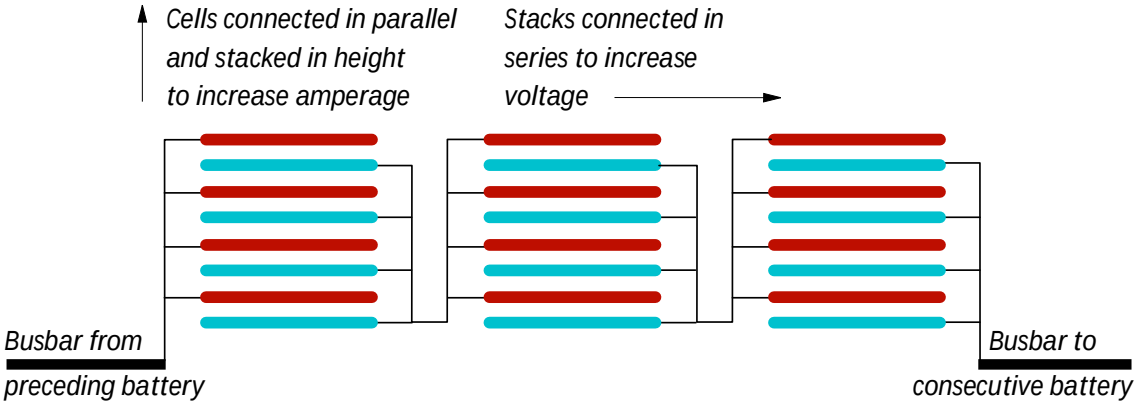

Figure 4. Stacking of individual battery cells.

4. Main Battery Construction and Capacity Estimates

In the following, we will analyse the distribution between battery current and rectifier current during discharge.

The following data were adopted for the estimates:

E_p = 1.7 x 250 = 425 V (1.2 V reversible voltage, 0.5 V activation overvoltage, 250 cells in series).
R_p = 2.70 x 10^{-3} Ω (250 cells in series, 250 kA, 4.4 V cell voltage).
E_b = 1.90 x 3 x 225 = 1282.5 V (1.90 V per battery cell at full charge (including 0.05 V activation overvoltage), 3 cells in series in each battery position, 225 battery positions).
R_b = 0.73 x 10^{-3} Ω (about 0.81 V ohmic losses per battery position at 250 kA, including voltage drop in busbars).

Figure 5 shows the battery current as a function of the voltage during discharge, also including other number of battery positions than the 225 positions mentioned above.

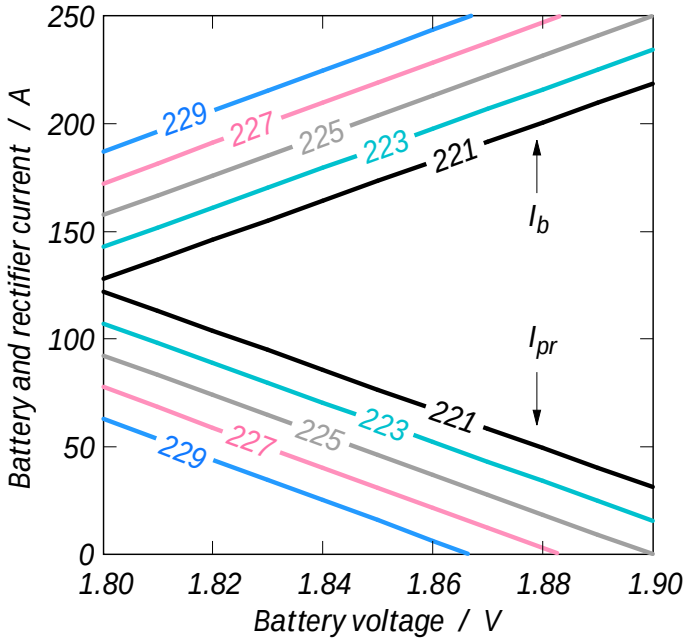

Figure 5. Battery and rectifier current (I_b and I_{pr}) as a function of the battery voltage (E_b) at different number of active battery positions.

The battery stack (Figure 4) could have small interpolar distance and very many cells, or large interpolar distance and fewer cells. In the first case, the stack will have large area and become relatively expensive. In the latter case, the voltage loss may be too high due to large interpolar distance as well as high current density. Also, the capacity of the battery depends on the number of cells in each stack, which will be estimated in the following.

4.1. Voltage Drop and Current Density

The footprint area of a 250 kA potshell may be about 45 - 50 m^2. In the following, each of the primary cells in the three stacks is assumed to cover 14 m^2. The ohmic voltage loss corresponds to 0.81 V per battery position at full load, including the busbars between the batteries. Taking the busbar voltage drop to be 0.25 V at 250 kA, the voltage drop across each primary cell in the three stacks becomes 0.19 V.

The voltage drop in the electrolyte is given by:

$$E_e = \frac{Ih}{AN\kappa} \tag{7}$$

Where: I *B*attery current (maximum 250 kA),
h Height of the electrolyte,
A Individual cell area (14 m^2),
N Number of parallel-connected cells in each stack and
κ *E*lectrical conductivity of the electrolyte.

The electrical conductivity of the electrolyte is not readily available for the system NaCl-$CaCl_2$-$ZnCl_2$. NaCl has a relatively high conductivity and $CaCl_2$ has an intermediate value. The conductivity of pure $ZnCl_2$ is very low, but it increases rapidly upon addition of NaCl [10]. In the binary system NaCl-$CaCl_2$, the variation with the composition is very non-linear [11]. In the present context, it will be regarded as good enough to assume that the conductivity is about 200

Sm^{-1} (it could be lower near the discharged state). By taking the maximum allowable electrolyte voltage drop to be 0.15 V at 250 kA, the above numbers inserted in Equation (7) yield:

$$h = 0.00168N \quad [\text{m}] \tag{8}$$

The current density (i) becomes:

$$i = \frac{17857}{N} \qquad [\text{A/m}^2] \tag{9}$$

As an example, a stack containing N = 20 cells must have h = 0.0336 m electrolyte in each cell, and the current density becomes 893 A/m^2.

4.2. Charge Capacity

The limiting factor for the battery capacity appears to be the amount of $ZnCl_2$ present in the lower electrolyte. For this reason, the height of the lower electrolyte should be kept higher than the upper electrolyte, to have maximum capacity and at the same time limiting the ohmic voltage drop.

The densities of binary and ternary mixtures of molten salts are not readily available. The densities of the pure salts at 900 K are as follows; NaCl: 1652 kg/m^3, $CaCl_2$: 2149 kg/m^3, and $ZnCl_2$: 2364 kg/m^3 [12]. The density does not vary linearly with the composition, due to complex formation. For the present purpose however, it is sufficient to assume a density of 2200 kg/m^3 at full charge. The $46ZnCl_2$-$54CaCl_2$ mixture then contains 9687 moles of $ZnCl_2$ per m^3, *i.e.*, 1.87 x 10^9 C/m^3 (519 kAh/m^3). The full theoretical capacity cannot be used however, due to reversible voltage limitations as well as limiting current for $ZnCl_2$ towards the end of discharge, and low transport number of Na^+ towards the end of charging. We assume that 70 percent of the theoretical capacity can be utilized without unacceptable efficiency losses, corresponding to 364 kAh per m^3 electrolyte on the zinc side. Furthermore, assuming that 70 percent of the total electrolyte volume is on the zinc side, the capacity based on the total volume becomes 255 kAh/m^3.

The total capacity of the battery (W_{el}) then becomes 255 kAh/m^3 multiplied with the electrolyte volume in each stack,

$$W_{el} = 255 \cdot A \cdot h \cdot N = 5.99 \cdot N^2 \quad [\text{kAh}] \tag{10}$$

4.3. Number of cells in each stack

The information given in Sections 4.1 and 4.2 above is summarised in Figure 6. As can be observed, a small number of cells in the stack gives small electrolyte height and high current density, but on the expense of the charge capacity. It is interesting that the charge capacity varies with the square of the number of cells in the stack (Equation (10)), which means that the capacity can be increased at relatively small cost. By using 20 cells in the stack, the charge capacity is 2.40 MAh, corresponding to 250 kA for 9.6 h. Provided that the electrolyte height constitutes not more than 50 percent of the total, the stack height will be less than 1.4 m, which can easily be accommodated inside a potshell.

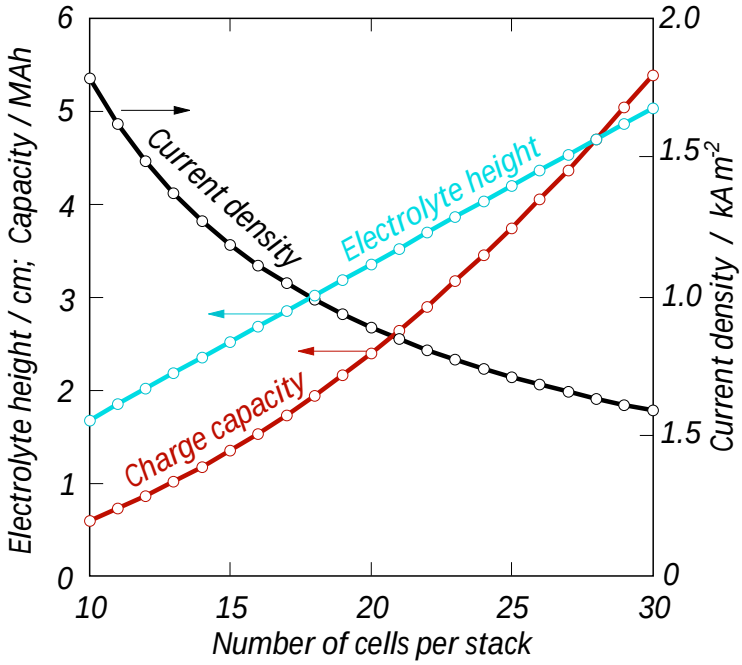

Figure 6. Electrolyte height, charge capacity, and current density as a function of the number of cells per stack. Electrical conductivity 200 S/m, electrolyte voltage drop 0.15 V at 200 kA, 70 percent of the electrolyte at the zinc side.

4.4. Unit Cell Construction

Figure 7 shows a possible construction of a unit cell in the battery. The zinc electrode current collector bar should have high electrical conductivity and must, of course, withstand molten zinc. It is possible that it should be supplied with ribs or grooves to slow down the magneto-hydrodynamic flow of zinc. Alternatively, a porous material could be placed in the zinc phase. Graphite is a candidate material for the collector bar.

The diaphragm should be corrugated and supplied with holes or slits for letting through the droplets of Zn-Na alloy formed in the sodium pool. Possibly, the slits can be omitted if there is good wetting between the alloy and the diaphragm material. The diaphragm material must be able to withstand the electrolyte as well as the Zn-Na alloy and dissolved metal. Currently, porous zirconia is being tested in our laboratory.

The lining must be able to withstand all the liquid phases in the cell, and it must be an electrical insulator. Steel or graphite are candidate materials, provided that it can be coated by some kind of insulating layer. It is possible to imagine a quartz lining with a back-up of a structurally more robust material. The insulation can then be any porous material able to withstand 900 K.

The sodium current collector bar can, possibly, be made of mild steel. The compatibility with the Na-Zn alloy will have to be considered. The collector bar must be supplied with ribs, in order to accommodate the volume changes in the system. The gas above the sodium pool must be vented out of the stack, and stored in a closed system to avoid air coming into the cell.

The cell separator is simply a sheet of insulating material. It will not be subjected to severe conditions, except the temperature.

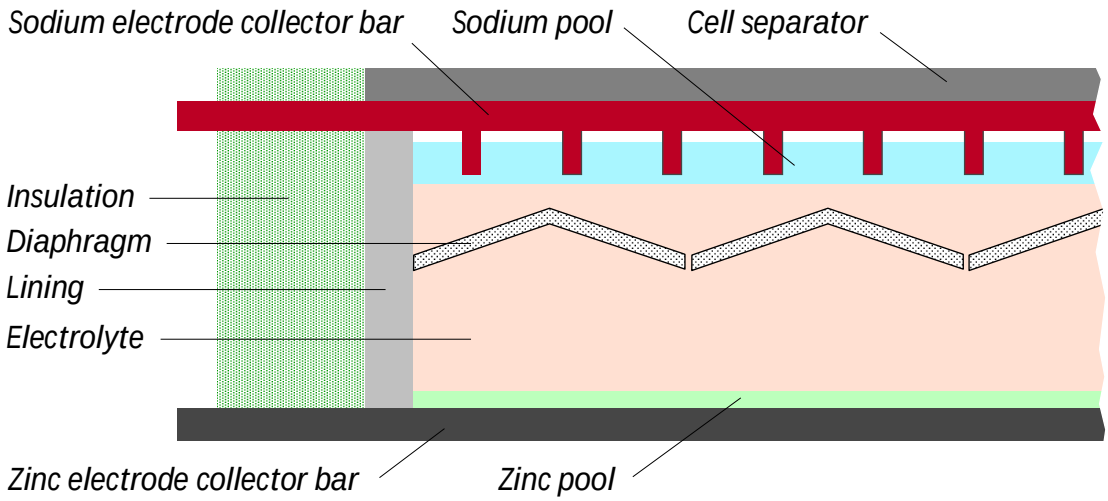

Figure 7. Possible construction of the battery (see the text).

4.4. Energy Balance

Like the aluminium electrolysis cells, the energy balance for the battery is delicate. The average heat evolution inside the battery must exactly match the heat loss during a charge/discharge cycle, without too much temperature variation.

There are two main classes of heat sources inside the battery, i) Joule heating and product of current and overvoltages, and ii) the product of current and the difference between the isothermal cell voltage and the reversible voltage (E^{iso}-E^{rev}).

The first class of heat source is independent of the current direction, and it is always positive. The second type of heat source corresponds to the entropic heating ($T\Delta S$). The reversible and isothermal voltages are negative during charging and positive during discharge. Since the absolute of E^{iso} (about 2.17 V) is larger than the absolute value of E^{rev} (about 1.9 V), the total entropic heating will be negative during charge and positive during discharge.

In a battery system without loss in current efficiency, the heat loss must exactly balance the heat sources of class i) above, while the entropy of the cell reaction gives temperature swing. Preliminary estimates indicate that managing the energy balance will not be a major challenge.

5. Concluding Remarks

A use case for using a liquid metal battery as a power buffer in an aluminium plant by locating the battery in an idled potline has been evaluated. The calculations show that with the assumptions made, it could hold enough charge capacity to supply the working potline for approximately 10 hours before it needs to recharge. It should be emphasized that the battery concept described in the present paper is still at a very early stage of development, and the cost picture has not been considered.

There is currently some concern about the magnetohydrodynamic (MHD) stability of grid-scale LMBs. Bojarevics and Tucs [13] analysed an LMB cell using the physical cell size and busbar configuration of the Trimet smelter as a starting point. It was found that the cell was MHD stable at 2 cm electrolyte height at a considerable higher current density than used in the present work. This may indicate that any MHD problems can be overcome by proper busbar design, in the same way as has been achieved for aluminium electrolysis cells.

6. Acknowledgement

The present work was performed within the project "Membrane free liquid metal batteries for grid scale energy storage", financed by the Research Council of Norway. Valuable input from and stimulating discussions with Christian Droste and Christian Rosenkilde, both Hydro Aluminium, is gratefully acknowledged.

7. References

1. H. Kim, D.A. Boysen, J.M. Newhouse, B.L. Spatocco, B. Chung, P. J. Burke, D. J. Bradwell, K. Jiang, A. A. Tomaszowska, K. Wang, W Wei, L.A. Ortiz, S.A. Barriga, S.M. Poizeau, and D.R. Sadoway: Liquid Metal Batteries: Past, Present, and Future, *Chem. Rev.* 113 (2013) 2075−2099 (dx.doi.org/10.1021/cr300205k).
2. J. Xu, O.S. Kjos, K.S. Osen, A.M. Martinez, O.E. Kongstein, and G.M. Haarberg: Na-Zn Liquid Metal Battery, *Journal of Power Sources* 332 (2016) 275-280.
3. ICIS, http://www.icis.com/resources/news/2016/05/09/9996090/deeply-negative-prices-return-to-rock-german-power-market/
4. P. Lavoie, S. Namboothiri, M. Dorreen, J.J.J. Chen, D.P. Zeigler, and M.P. Taylor: Increasing the Power Modulation Window of Aluminium Smelter Pots with Shell Heat Exchanger Technology, *Light Metals* 2011, 369-374.
5. R.P. Pawlek: Primary Aluminium Industry in the year 2016, *Light Metal Age* 75 (1) (2017) 8-21.
6. HSC Chemistry 7, ver 7.11, © Outotec Research Centre (www.outotec.com)
7. D.R. Flinn and and K.H. Stern: Electrochemical Properties of Sodium Beta-Alumina in $ZnCl_2$ - NaCl Melts, *J. Electrochem. Soc.* 123(7) (1976) 978-981.
8. H. Cetin and R.G. Ross: The Phase Diagram of Na-Zn Alloys", *Journal of Phase Equilibria* 12 (1) (1990) 6-9 (DOI: 10.1007/BF02663664).
9. C. Robelin and P. Chartrand: Thermodynamic Evaluation and Optimization of the (NaCl + KCl + $MgCl_2$ + $CaCl_2$ + $ZnCl_2$) System, *J. Chem. Thermodynamics* 43 (2011) 377-391.
10. B. Kubikova, M. Simurda, E. Robert, Z. Shi, and M. Boca: Surface Tension, Electrical Conductivity, and Viscosity of the LiCl-NaCl-$ZnCl_2$ System, *Journal of Molecular Liquids* 224 (2016) 672-676.
11. Z. Chen, J. Liu, Z. Yua, K.-C. Choua: Electrical Conductivity of $CaCl_2$-KCl-NaCl System at 1080 K, *Thermochimical Acta* 543 (2012) 107-112.
12. Anonymous, http://moltensalt.org/references/static/downloads/pdf/element-salt-densities.pdf
13. V. Bojarevics and A. Tucs: MHD of Large Scale Liquid Metal Batteries, *Light Metals* 2017, 697-692.